Homogeneously-alloyed CdTeSe single-sized nanocrystals with bandgap photoluminescence

Wang, Ruibing; Calvignanello, Olivier; Ratcliffe, Christopher I.; Wu, Xiaohua; Leek, Donald M.; Zaman, Md. Badruz; Kingston, David; Ripmeester, John A.; Yu, Kui

Publisher's version / Version de l'éditeur:
https://doi.org/10.1021/jp810325z
The Journal of Physical Chemistry, 113, 9, pp. 3402-3408, 2009-02-10

THE JOURNAL OF PHYSICAL CHEMISTRY C

Article

Homogeneously-Alloyed CdTeSe Single-Sized Nanocrystals with Bandgap Photoluminescence

Ruibing Wang, Olivier Calvignanello, Christopher I. Ratcliffe, Xiaohua Wu, Donald M. Leek, Md. Badruz Zaman, David Kingston, John A. Ripmeester, and Kui Yu

J. Phys. Chem. C, **2009**, 113 (9), 3402-3408• DOI: 10.1021/jp810325z • Publication Date (Web): 10 February 2009

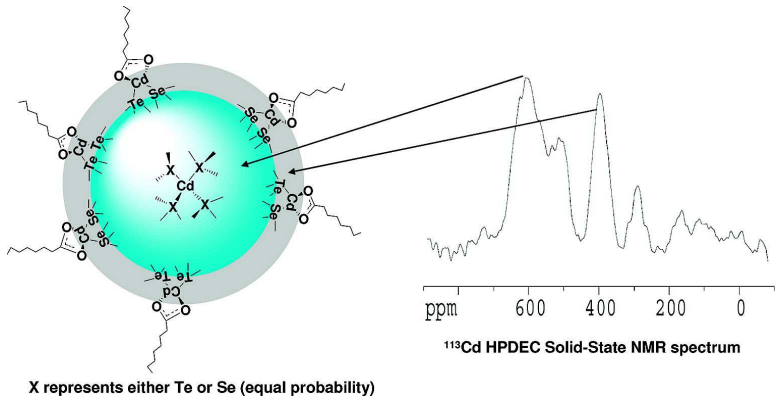

More About This Article

Additional resources and features associated with this article are available within the HTML version:

- Supporting Information
- Access to high resolution figures
- Links to articles and content related to this article
- Copyright permission to reproduce figures and/or text from this article

View the Full Text HTML

The Journal of Physical Chemistry C is published by the American Chemical Society. 1155 Sixteenth Street N.W., Washington, DC 20036

Homogeneously-Alloyed CdTeSe Single-Sized Nanocrystals with Bandgap Photoluminescence

Ruibing Wang,[†] Olivier Calvignanello,[†] Christopher I. Ratcliffe,[†] Xiaohua Wu,[‡] Donald M. Leek,[†] Md. Badruz Zaman,[†] David Kingston,[§] John A. Ripmeester,[†] and Kui Yu*,[†]

Steacie Institute for Molecular Sciences, Institute for Microstructural Sciences, and Institute for Chemical Process and Environmental Technology, National Research Council of Canada, Ottawa, Ontario K1A 0R6, Canada

Received: November 24, 2008; Revised Manuscript Received: December 28, 2008

Homogeneously alloyed ternary CdTeSe magic-sized nanocrystals (MSNs) with bandgap emission were synthesized in 1-octadecene (ODE) via a noninjection one-pot approach featuring synthetic reproducibility and large-scale capability. The noninjection approach used cadmium acetate dihydrate ($Cd(OAc)_2 \cdot 2H_2O$), elemental selenium, and elemental tellurium as Cd, Se, and Te sources, respectively. The growth of the CdTeSe nanocrystals was carried out at temperatures from 120 to 200 °C for several hours in a reaction flask containing the reactants together with a long-chain fatty acid as capping ligands and ODE as the reaction medium. During synthesis, the CdTeSe nanocrystals exhibited persistent bandgap and did not grow in size anymore after their formation, either with longer growth periods or higher reaction temperature. Also, they exhibit an absorption doublet with 288 meV energy difference between the two peaks; the first excitonic transition peak is at 520 nm and bandgap photoemission peak at 524 nm with full width at half-maximum (fwhm) of ca. 20 nm. Both the growth pattern and the optical properties suggest that they are magic-sized and thus termed as single-sized. Nuclear magnetic resonance (NMR), with sensitivity to local environment, provided valuable information regarding the structure and composition of the nanocrystals. Solid-state ^{13}C cross polarization/magic angle spinning (CP/MAS) NMR spectra showed that the carboxylate capping ligand is firmly attached to the crystal, and ^{1}H decoupled ^{113}Cd MAS spectra, with and without CP, distinguished between the surface Cd species and the Cd inside a nanocrystal. The ^{113}Cd NMR results also confirmed, unambiguously, that the nanocrystals are homogeneously alloyed ternary CdTeSe, with ^{113}Cd resonances located between those of CdTe and CdSe nanocrystals indicating a stoichiometry of approximately 1Se:1Te ratio throughout the whole nanocrystal. XRD supported that they are ternary-alloyed CdTeSe rather than binary CdTe or CdSe, with a wurtzite crystal structure. In addition, both energy-dispersive X-ray spectroscopy (EDX) and X-ray photoelectron spectroscopy (XPS) supported an approximate stoichiometric ratio of 1Se:1Te of the CdTeSe nanocrystals.

1. Introduction

Colloidal semiconductor quantum dots (QDs) exhibiting bandgap photoemission have generated a great deal of interest in both fundamental sciences and technological applications for the past decade, owing to their unique optical properties such as narrow emission with broad absorbance and good photostability.[1−3] The size-dependent bandgap absorption and emission of colloidal QDs is of particular interest. However, significant complications arise in the study of their fundamental physics, because the variation in size within one ensemble sample leads to inhomogeneous spectral broadening and thus a loss of single-dot spectral information from averaging.[4,5] (The terms "homogeneous" and "inhomogeneous" spectral broadening were used to refer to the optical properties without and with size distribution, respectively.)[4] Meanwhile, for many potential applications such as biolabeling,[1,2] multiplexed bar-coding,[3] optoelectronic devices,[6] and lasers where narrow emission provides high energy density at specific wavelengths and therefore imparts more efficient conversion of pump power into a single mode emission,[7,8] there are outstanding needs for QD ensembles exhibiting narrow emission bandwidth.

Progress has been made in achieving various colloidal QD ensembles, with a certain degree of control in size distribution and thus bandgap emission bandwidth.[9−12] Hot-injection approaches are the most successful and widely used to engineer colloidal QD ensembles with narrow emission bandwidths; however, such approaches are not ready for industrial-scale production. On the other hand, noninjection approaches are better suited for large-scale production.[12] Meanwhile, challenges still remain in synthesizing colloidal QD ensembles exhibiting single-dot optical properties, particularly bandgap emission. A single-sized QD ensemble, namely without size distribution, could exhibit single-dot optical properties free of inhomogeneous spectral line broadening. Furthermore, with proper surface passivation, such an ensemble could be expected to produce bandgap emission. Therefore, for one colloidal QD ensemble with bandgap emission, the narrowest bandwidth would be realized when the ensemble is single-sized and thus without inhomogeneous spectral broadening.

Single-sized quantum dots, also referred to as "magic-sized quantum dots" (MSQDs) (including "magic-sized nanoclusters")

* To whom correspondence should be addressed. E-mail: kui.yu@nrc-cnrc.gc.ca.
[†] Steacie Institute for Molecular Sciences.
[‡] Institute for Microstructural Sciences.
[§] Institute for Chemical Process and Environmental Technology.

10.1021/jp810325z CCC: $40.75
Published on Web 02/10/2009

have been reported.[13−23] During synthesis, the most direct identification of the presence of MSQDs was the occurrence of persistent absorbance without red-shift. Furthermore, they were suggested to have a fixed size, shape, and composition with precision on the atomic level.[14,18,21] Thus, they exhibit absorption without inhomogeneous spectral broadening but with only homogeneous spectral broadening.[4] In fact, they were discovered as molecular cluster-like precursors leading to the formation of larger aggregates with various morphologies such as wire-like.[13−16] It is noteworthy that, for those II−VI MSQDs reported,[17−22] they exhibited no bandgap but trap emission; and very often, several families of different sizes coexisted in one synthetic batch.[19,20] It was not until recently that PbSe MSQDs were claimed to have bandgap emission, but unfortunately with broad bandwidth,[23] which might result from the nature of the broad homogeneous fluorescence line width.[23,24] However, the synthesis reported did not achieve any MSQD ensemble in pure form but with the coexistence of multiple families.[23]

It is noteworthy that MSQD ensembles and regular QD (RQD) ensembles exhibit significantly different optical properties. For the case of CdSe, a MSQD ensemble demonstrates single-dot optical properties including narrow bandwidth of ca. 10 nm measured as full width at half-maximum (fwhm) and small nonresonant Stokes shift (NRSS), due to the fixed size, shape, structure, composition with an atomic precision, good surface passivation, and its intrinsic exciton fine structure.[4,25] On the other hand, even with the minimum size distribution of 5%, a regular CdSe QD ensemble exhibits larger than 25 nm fwhm of bandgap emission, due to inhomogeneous spectral broadening.[9−12]

The most recent advance is that three CdSe magic-sized quantum dots (MSQD) families exhibiting bandgap emission were synthesized in pure form in our laboratories via a newly developed one-pot noninjection approach.[25] This approach is simple, featuring high synthetic reproducibility and large-scale production, using cadmium acetate dihydrate ($Cd(OAc)_2 \cdot 2H_2O$) and elemental selenium as Cd and Se sources, respectively, a fatty acid as surface ligands, and 1-octadecene (ODE) as the reaction medium. Upon modification of this facile noninjection approach, one CdTe MSQD ensemble exhibiting bandgap emission with fwhm of ca. 10 nm only was synthesized in pure form, and several larger families exhibiting bandgap emission were also engineered.[26]

Inspired by our achievements on the binary CdSe and CdTe MSQDs, and considering the fact that there has been no ternary-alloyed CdTeSe MSQDs reported, we have expanded our efforts in this direction. Here, we report one small alloyed-ternary CdTeSe MSQD ensemble in pure form exhibiting bandgap absorption at 520 nm and bandgap photoemission at 524 nm with fwhm of ca. 20 nm only. This ensemble, named as Family 524 according to its bandgap emission peak position in nm, was synthesized via a noninjection one-pot approach. The growth kinetics, stability in size, and optical properties of the nanocrystals suggest that they are single-sized. Detailed characterization, including solid-state NMR, TEM, EDX, XPS, and PXRD, was performed on the resulting CdTeSe MSQD ensemble, leading to unique insights on the structure and composition of the ternary MSQDs, which are homogeneously alloyed rather than gradiently alloyed ternary QDs with an approximate 1Se:1Te stoichiometric ratio.

2. Experimental Section

2.1. Synthesis of CdTeSe Nanocrystals. In a typical synthesis, the Cd precursor Cd(acetate)(octate) was made in situ by mixing equimolar cadmium acetate (0.32 mmol) and octanoic acid (0.32 mmol) in 4.0 g of 1-octadecene (ODE) for 2 h at 120 °C under vacuum (to remove acetic acid). Meanwhile, the precursors TOPSe and TOPTe were freshly prepared together by sonicating 0.04 mmol of elemental Se and 0.04 mmol of elemental Te in about 0.1 g of TOP (minimum possible) at 60 °C for 2 h. The solution of TOPSe and TOPTe in TOP was thereafter transferred into the Cd precursor solution prepared; and the sonication container was rinsed with about 0.9 g of ODE to maintain ca. 5.0 g of the total solvent (consisting of ODE and TOP) in the reaction flask. For the growth of CdTeSe MSQD Family 524, the reaction mixture was kept at 120 °C for 1 h, and then, the temperature was increased slowly to 180 °C at a rate of ca. 2 °C/min under a flow of Ar. The growth was monitored by the temporal evolution of the optical properties of the growing nanocrystals (as shown in the Supporting Information, Figure S1). Optical absorption spectra were collected with a Perkin-Elmer Lambda 45 ultraviolet−visible (UV−vis) spectrometer using a 1-nm data collection interval. Photoemission experiments were performed on a Fluoromax-3 spectrometer (Jobin Yvon Horiba, Instruments SA), with a 450 W Xe lamp as the excitation source, an excitation wavelength of 350 nm (if not specified), an increment of data collection of 1 nm (if not specified), and the slits of 3 nm (if not specified).

2.2. Sample Purification for NMR, XRD, and TEM/EDX. Solid-state nuclear magnetic resonance (NMR), powder X-ray diffraction (XRD), and transmission electron microscopy (TEM) including EDX characterization require intensive sample purification, to avoid interfering signals from the reaction mixture including ODE, TOP, unreacted species, and other side products of the reaction. For the purification, the as-synthesized nanocrystal ensemble was centrifuged first at 4000 RPM for 25 min to obtain brown-color precipitate; afterward, the resulting precipitate was washed three times with toluene/methanol (1:1). Diffusion-ordered spectroscopy (DOSY) NMR experiments require less intensive washing as the signals from chemicals such as ODE, toluene, and the unreacted species normally do not create confusion on the interpretation of the nanocrystal size. The sample for solution NMR was only washed once in order to reduce the degree of possible aggregation.

2.3. Characterization with NMR, XRD, and TEM/EDX. Solid-state NMR spectra were obtained on a Bruker AMX300 spectrometer with a Doty Scientific Inc. 5 mm probe using silicon nitride rotors. Standard ^{13}C cross polarization/magic angle spinning (CP/MAS) spectra at 75.43 MHz were obtained with a CP time of 2 ms, and 2 s recycle times, and dipolar dephasing spectra were obtained with an interruption of ^{1}H decoupling of 40 μs before data acquisition (referenced to TMS via external hexamethylbenzene). ^{113}Cd NMR magic angle spinning (MAS) spectra with ^{1}H high power decoupling were obtained at 66.58 MHz, both with and without ^{1}H cross-polarization (CP). For ^{113}Cd spectra without CP, a simple high power proton decoupled (HPDEC) sequence with phase cycling was used, with a 90° pulse length of 4.0 μs, and a recycle time of 120 s which required collection times of the order of 3 days. ^{113}Cd CP/MAS spectra were obtained with a recycle time of 2 s, and a CP time of 5 ms for optimum signal, though spectra with other CP times were also obtained. Chemical shifts were referenced to $Cd(NO_3)_2 \cdot 4H_2O$ (powdered, under CP/MAS). Spin rates were 6.9−7.1 kHz.

For the nanocrystal size, the solution NMR analyses were performed using a Bruker DRX-400 spectrometer equipped with an inverse detected Z-gradient probe. Diffusion coefficients were measured by the DOSY-NMR experiment using standard Bruker

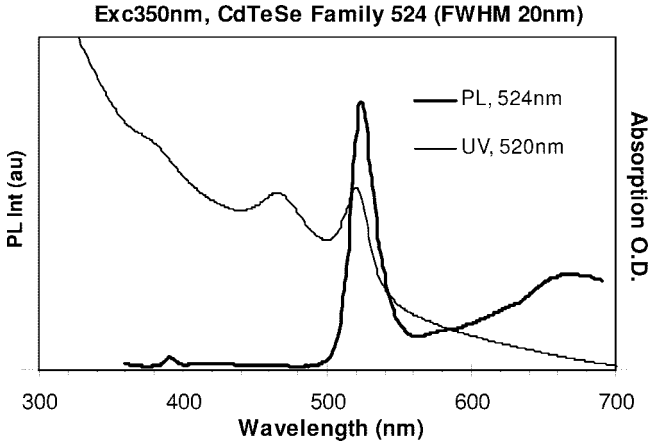

Figure 1. Emission (thick line, left *y* axis) and absorption (thin line, right *y* axis) spectra of the as-synthesized CdTeSe alloyed MSNs, whose growth was at 180 °C.

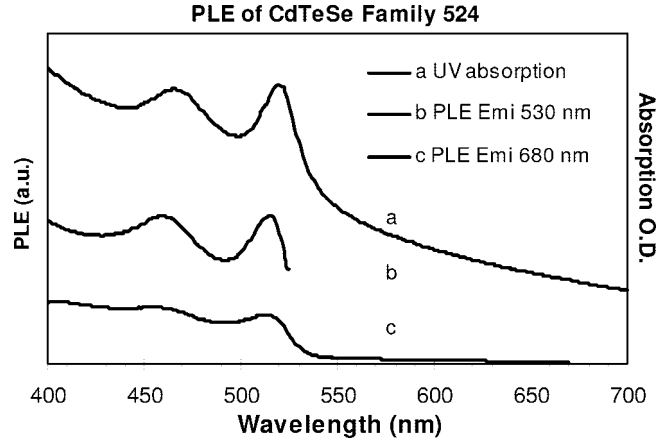

Figure 2. Photoluminescent excitation (PLE) spectra of one F524 sample dispersed in toluene, with the emission at 530 nm (b) and at 680 nm (c), together with UV absorption spectrum (a).

pulse sequences. Heptakis-(2,3,6-tri-*o*-methyl)-β-cyclodextrin, which has an average diameter of 1.4 nm, was used as an internal standard. According to the Stokes−Einstein equation, the diffusion coefficient of a particle is inversely proportional to its diameter. The size of the nanoparticles was calculated from the ratio of their diffusion coefficients to that of the internal standard. The use of an internal standard eliminates the need for accurate knowledge of the parameters such as the sample viscosity and the temperature.

Powder XRD pattern of the sample was acquired at room temperature on a Bruker Axs D8 X-ray diffractometer using Cu Kα radiation in a $\theta-\theta$ mode. The generator was operated at 40 kV and 40 mA, and data were collected between 5° and 75° in 2θ with a step size of 0.1° and a counting time of 5 s per step. The XRD sample was prepared by depositing the purified nanocrystals on one low-background quartz plate.

TEM was performed on a JEOL JEM-2100F electron microscope operating at 200 kV and equipped with a Gatan UltraScan 1000 CCD camera. The sample was prepared by drying one drop of dilute purified MSQD dispersion in toluene onto a 300-mesh carbon-coated TEM copper grid. EDX measured was carried out on the same set of TEM instrument, equipped with EDS system (the Oxford Instrument INCA Energy TEM 200) for EDX measurement. The spectra from six different areas of the sample were acquired at 0−20 keV scale and analyzed by the on-site software.

3. Results and Discussion

Figure 1 shows the absorption and emission spectra of the as-synthesized ternary CdTeSe MSQDs with the growth temperature of 180 °C. This MSQD CdTeSe Family 524 exhibits a sharp absorption doublet with its first excitonic transition peaking at 520 nm, and bandgap emission at 524 nm with narrow fwhm of ca. 20 nm. Note that the absorption and emission maxima of the MSQD ensemble are independent of the growth periods during the reaction (as shown in the Supporting Information, Figure S1), implying stability in size with a constant bandgap; the growth pattern shows the typical characteristics of MSQDs.[13−23] Furthermore, if the reaction temperature was increased up to 240 °C, Family 524 was thermally stable without further growth in size, as indicated by the absence of redshift in absorption and emission.

Similar to that of previously reported for CdSe MSQDs,[25] the absorption doublet may represent also the two electronic transitions but with the energy difference of ca. 288 meV: 1S(e)-$1S_{3/2}$(h) the lowest transition at 520 nm and 1S(e)-$2S_{3/2}$(h) the second lowest at 464 nm. Note that CdSe MSQD Family 395, Family 463, and Family 513, and CdTe MSQD Family 428, which were all synthesized in pure form, exhibit similar absorption doublets, with the energy difference between the two transitions of ca. 185, 173, 161, and 308 meV, respectively.[25,26] Thus, the value of the energy difference of the present absorption doublet of the CdTeSe MSQDs is larger than those of the CdSe MSQDs and smaller than that of the CdTe MSQDs. Such a difference in the value of the energy difference of the absorption doublet suggests that the present MSQDs represent a ternary system.

Furthermore, the fwhm of ca. 20 nm of the bandgap emission is dramatically smaller than the smallest value of 35 nm claimed (but typically 50 - 60 nm in the spectra shown) previously for a ternary-alloyed CdTeSe regular QD ensemble synthesized by a 300 °C hot-injection approach.[27,28] It is worthy of notice that homogeneous fluorescence linewidths of different semiconductor nanocrystals are different; CdSe and PbS single dots exhibit ca. 10 nm[4] and 50 nm[24] fluorescence line widths with homogeneous broadening, respectively. Therefore, it is reasonable that the CdTeSe MSQDs exhibit larger homogeneous fwhm than the binary CdTe and CdSe MSQDs. The ternary CdTeSe regular QDs were reported to have typical fwhm of 35−60 nm.[27,28]

Accordingly, the combination of the sharp absorption doublet with the energy difference of 288 meV, narrow emission with 20 nm fwhm, ultrasmall NRSS, and growth kinetics with the size stability based on the constant bandgap monitored during the reaction suggests the presence of a magic-sized ensemble. The quantum yield was estimated to be ca. 1%; with such a narrow emission bandwidth, the emission was "bright" with high intensity. Such bandgap emission is a significant achievement compared with the previously reported MSQDs without bandgap emission.[20−22] In addition to the bandgap emission, the broad emission at lower energies is due to deep trapping, as proved by the photoluminescence excitation spectrum shown in Figure 2c (in a comparison with the UV−vis absorption spectrum). Such deep trap emission is indicative of the presence of defects including incomplete surface passivation. Efforts to eliminate the trap emission are ongoing in our laboratories. Note that the nonflat baseline of the absorption spectrum shown in Figures 1 and 2 may be related to the aggregation of the ultrasmall and single-sized nanocrystals in toluene;[16] sonicaton was attempted to reduce the aggregation but with little effect.

NMR is a powerful tool for structural and compositional characterization, providing information about the local environ-

ments of nuclei in different sites as reflected in their chemical shifts. Solid-state NMR techniques including CP/MAS have been used to study semiconductor quantum dots (QDs), such as the surface reconstruction with local structural changes from surface to core of InP nanocrystals by Alivisatos and co-workers,[29] the surface reconstruction of hexadecylamine-capped CdSe nanocrystals with a wurtzite crystal structure by Strouse and co-workers,[30] and the surface structure distinguished from core structure of CdS nanocrystals by Elbaum et al.[31,32] Also, solid-state NMR has been used to study the structure of doped lanthanum fluoride (LaF_3) nanocrystals via probing the distribution of the dopants through the nanocrystals and the nature of the ligands and their interaction with surface atoms by Veggel, Schurko, and co-workers,[33] and the coordination of phosphonic acids to the surface of SnO_2 nanoparticles by Holland, Yarger, and co-workers.[34] Previously we also reported solid-state NMR studies of the synthesis-structure−property relationship of ternary-alloyed regular QDs of CdTeSe with TOP capping agents and ZnCdS regular QDs with stearic acid capping agents.[28,35] The interactions of the surface ligand and surface Cd atoms were identified, together with the structural information of the ternary core, namely homogeneously alloyed vs gradiently alloyed. To the best of our knowledge, our solid-state NMR identification of such structural information of ternary QDs, including the surface environment and inner chemical composition, was the first.[28,35] Therefore, solid-state NMR has been successful and powerful in the structural and compositional characterization of QDs and has become a reliable tool to examine the surface and the core of nanocrystals: the former includes the nature of the binding between surface atoms and ligands and surface reconstruction with structural changes from surface to core; the latter includes the composition and compositional change of the core of nanocrystals.

The structure and composition of the brand-new ternary CdTeSe MSQDs have been studied in detail by solid-state NMR, with the composition result in good agreement with EDX and XPS. Figure 3 shows solid-state ^{113}Cd CP/MAS (A) and ^{113}Cd HPDEC (B) NMR spectra of CdSe MSN Family 463, CdTeSe MSQD Family 524, and CdTe MSQD Family 428. Similar to our previous work,[35] the ^{13}C CP/MAS spectra (shown in the Supporting Information, Figure S3) and the ability to obtain ^{113}Cd CP/MAS NMR suggest that the fatty acid used to passivate the MSQDs is firmly attached to the surface of the nanocrystals, presumably as carboxylate anions; otherwise cross-polarization from the protons of the alkyl chains of the ligands to the Cd would not be possible. The surface Cd atoms are strongly emphasized in the ^{113}Cd CP/MAS spectra (3A), whereas the HPDEC spectra (3B) show all the Cd, thus allowing signals from surface and core to be distinguished.[31,32,35]

All three MSQD samples show the same type of spectra consisting of two resonances, as summarized in Table 1: (a) The resonance at larger shifts (indicated by circular symbols) is weaker in the CP spectra and its lack of significant spinning side-bands (ssb) indicates a relatively isotropic environment. On this basis and by comparison with the shifts for bulk CdSe and CdTe,[28] this resonance can be assigned to core Cd tetrahedrally coordinated by four chalcogenide atoms. (b) The second resonance (indicated by square symbols) is prominent in both CP and HPDEC spectra and can therefore be assigned to surface Cd species. It also shows several strong ssb indicating a large chemical shift anisotropy. This site is therefore much less symmetric than the Cd core sites. It is surprising that there are only two signals, as this implies a sudden change from core to surface Cd with no intermediate state.

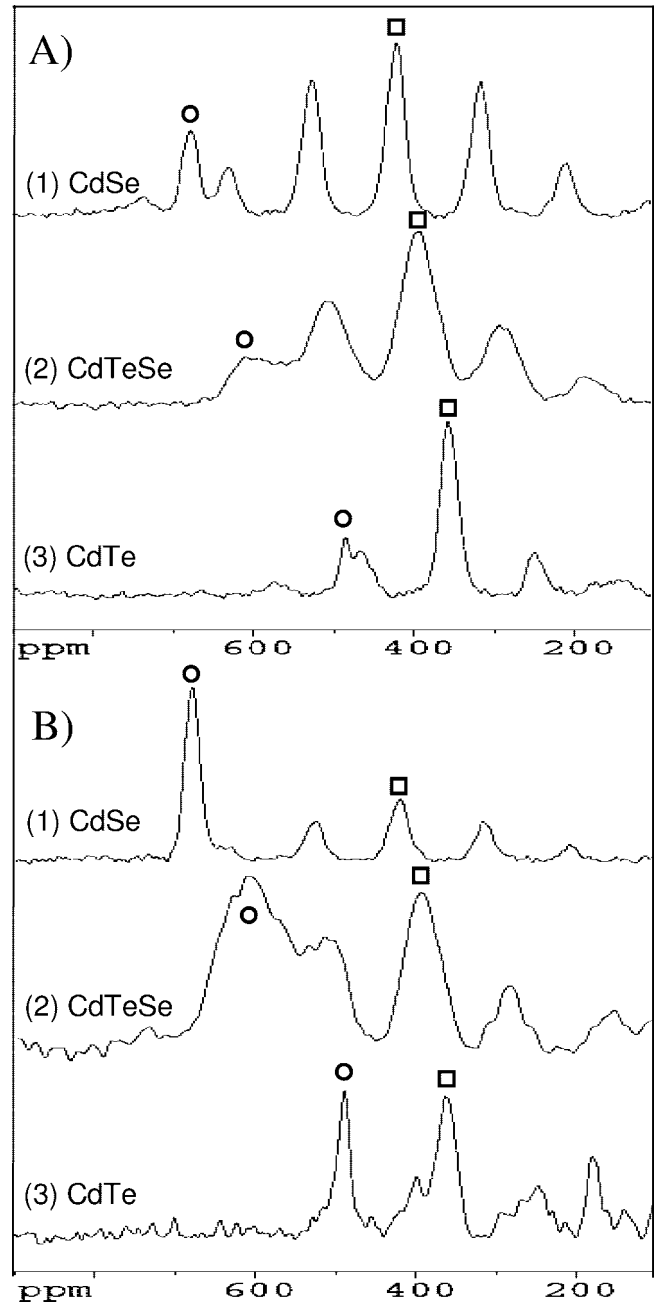

Figure 3. Solid-state ^{113}Cd CP/MAS (A, with 5 ms CP) and HPDEC (B) NMR spectra of CdSe (1), CdTeSe (2), and CdTe (3) MSNs. Circles indicate the ^{113}Cd resonance arising from core Cd atoms, whereas squares indicate the isotropic line of ^{113}Cd CP resonance from surface Cd atoms. Note that the unlabeled resonances on the sides of labeled peaks are spinning side bands.

TABLE 1: ^{113}Cd CP/MAS and HPDEC Solid-State NMR Chemical Shifts of the CdTeSe MSQDs via Our Noninjection One-Pot Approaches[25,26]

	core (circles)	surface (squares)
CdSe	680	422
CdTeSe	604	394
CdTe	485	357

The isotropic shifts for both the core and surface resonances decrease in the order CdSe, CdTeSe, and CdTe; also, for the CdTeSe MSQDs, the shifts for both core and surface are close to the median values between CdSe and CdTe MSQDs. It is of help to point out that, as shown in Figure 3B, CdSe Family 463 and CdTe Family 428 exhibit core ^{113}Cd at 680 and 485

ppm, respectively; thus, a mixture of both families would give only the same two separate resonances of core Cd, without signals between 680 and 485 ppm. Consequently, Figure 3B-2 is, unambiguously, from a ternary-alloyed CdTeSe system rather than from a mixture of binary systems of CdSe and CdTe. Also, the CdTeSe MSQDs are homogeneously alloyed and not gradiently alloyed since the latter would be expected to give much broader lineshapes.[28] For the composition of the CdTeSe nanocrystal core, assuming a roughly linear dependence of the shift on the Se-to-Te atomic ratio, the CdTeSe composition is also estimated to be approximately 1Se:1Te ratio throughout the whole nanocrystal.

It is necessary to point out that both the core and surface ^{113}Cd resonances of the alloyed CdTeSe MSQDs are significantly broader than those of the pure CdSe and CdTe MSQDs. For the core Cd, such broadness is due to a statistically weighted distribution of site types, namely there are $CdSe_4$, $CdSe_3Te$, $CdSe_2Te_2$, $CdSeTe_3$, and $CdTe_4$, each with a distinct resonance line broadened further by distributions in second neighbor chalcogenides. Resonances for all these species overlap to produce the broad line which is observed.

For the surface Cd, several possibilities can be considered for the number of chalcogenide atoms bonded to each Cd and the resulting ^{113}Cd NMR spectra these would be expected to give: (a) with one bond there could only be two distinct Cd types LCdSe or LCdTe with statistical weights 1:1 (where L represents an unspecified number of carboxylate anions), giving two NMR resonances roughly at the shifts of those for pure MSQDs of CdSe and CdTe; (b) with two bonds there would be three distinct Cd sites, LCdSe2, LCdSeTe or LCdTe2, statistically weighted 1:2:1, in which case there would again be two resonances roughly at the positions of those for pure MSQDs of CdSe and CdTe and a third roughly midway between; (c) with three bonds there would be four types, LCdSe3, LCdSe2Te, LCdSeTe2, or LCdTe3 with statistical weights 1:3:3:1, and four resonances. In case (a) the two peaks should still be well resolved and thus, since this is not observed, we can rule out this possibility, whereas in cases (b) and (c) the lines would overlap to give a single broadened peak, so either of these is consistent with the observed spectra.

We can tentatively suggest, however, that case (c) is less likely than (b) based on the following reasoning: Note that for the core Cd signals when 4Se are replaced by 4Te the shift reduces by 195 ppm. Then for the surface Cd signals, in case (c) replacing 3Se with 3Te might be expected to reduce the shift by about $195 \times 0.75 = 146$ ppm, whereas in case (b) replacing 2Se with 2Te might be expected to reduce the shift by about 97 ppm. The latter is much closer to the observed change in shift of 65 ppm. Furthermore, if a surface Cd is attached to only two chalcogenide atoms, this would require a charge balance of -1, which can be provided by one carboxylate anion, suggesting that this anion is the surface ligand and not the acid molecule. The crystal structures of carboxylate salts of Cd frequently show the anions as chelating ligands, so this may be the preferred mode, though some structures show additional coordination of a carboxylate oxygen to a second Cd.[36−39] Accordingly, this all leads to a model of the probable surface structure of the CdTeSe MSQDs where Cd is attached into the body of the nanocrystal by bonds to two chalcogenides and attached to both oxygen atoms of a carboxylate anion.

Energy dispersive X-ray emission spectra (EDX) were measured to study the elemental composition of the CdTeSe MSQDs. Figure 4 shows a typical EDX spectrum obtained at 0−20 kV, along with peak assignments for Cd, Se, and Te

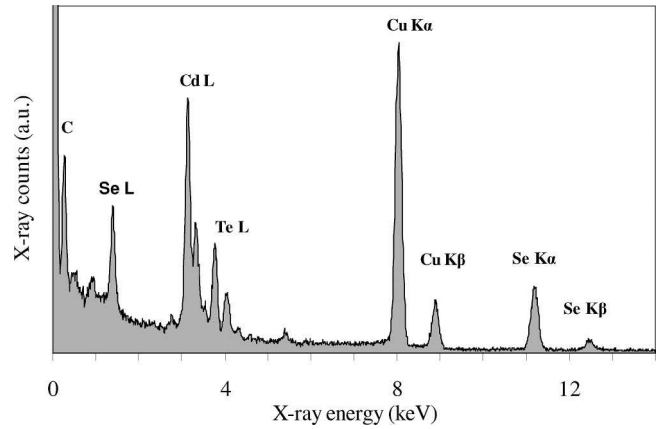

Figure 4. Energy dispersive X-ray (EDX) emission spectrum of homogeneously alloyed CdTeSe nanocrystals. Se-K, Cd-L, and Te-L were used for the quantification. Note that the Se-L was not used to avoid the contribution from the baseline in that area.

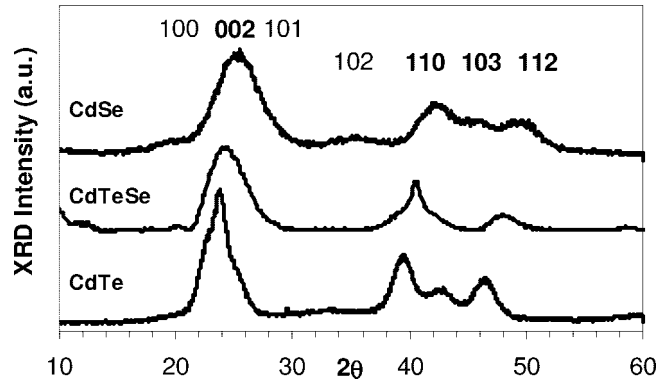

Figure 5. X-ray diffraction pattern of the CdTeSe ternary MSN Family 524 (middle), in comparison with those of CdSe (top) and CdTe (bottom) regular nanocrystal ensembles. The diffraction peaks are indexed.

elements. After integrating the peak areas of Cd-L, Te-L, and Se-K, we converted the X-ray counts into the elemental weight percentages using our quantification software (Oxford Instrument INCA Energy TEM 200 system). The resulting stoichiometric ratio of elements Cd: Se: Te was found to be 56:22:22, which is the averaged value from 6 scans from different areas of the sample, as shown in the Supporting Information, Figure S4, with the standard deviation of only ca. 2% (as shown in the Supporting Information, Table S1). Note that the ratio Cd: (Se+Te) is significantly greater than 1. The excess of Cd can be explained by the model of the surface where the Cd is attached to the core by two Se/Te and the other two Se/Te have been replaced by carboxylate. The 1Se:1Te stoichiometric ratio from the EDX results is also in agreement with the solid-state NMR result. Due to the fact that similar results on the Cd-to-Te-to-Se stoichiometric ratio were obtained from different spots of the TEM-EDX sample (as shown in the Supporting Information, Table S1 and Figure S4), the stoichiometric excess of Cd atoms should be representative of the nanocrystals. Please note that the EDX sample was washed three times intensively by toluene/methanol to remove unreacted species. More importantly, no ^{113}Cd NMR resonance from the Cd precursor was observed in the high-field region of the spectra of the CdTeSe MSQD sample.

The powder XRD of MSN Family 524 shown in Figure 5 also confirms that this ensemble is ternary CdTeSe, with diffraction peaks (2θ angles) situated between those of CdSe and CdTe regular QD ensembles. Furthermore, Family 524

reveals a wurtzite hexagonal structure, as compared to the XRD patterns of the wurtzite regular CdSe and CdTe QDs prepared previously.[28] High-resolution TEM images (as shown in the Supporting Information, Figure S5) of this Family 524 have shown well-resolved crystal lattice fringes, demonstrating the highly crystalline nature of these nanocrystals. Both XRD and TEM suggest a high degree of aggregation during the sample preparation; thus, they are inconclusive to characterize size and size distribution. Note that nearly all reported MSQDs by far are either too small to be seen by TEM[16] or tend to form aggregate so that their TEM images do not represent their actual sizes.[18−23,25,26] In fact, the aggregation tendency of CdSe MSQDs even facilitated the fabrication of ultranarrow quantum wires.[16]

For the size measurement of MSQDs in dispersion, both dynamic light scattering[23] and diffusion-ordered NMR spectroscopy (DOSY)[25,26] were reported to show little effect from the presence of ODE or other unreacted species; thus, intense sample purification is not demanded. There are reports on DOSY employed to study regular QD sizes[40] and the surface ligand affinity on the QD surface.[41] Therefore, the DOSY technique was used to determine the size of the CdTeSe MSQDs. The size is calculated to be 2.3 ± 0.5 nm, based on the value of their surface ligand diffusion coefficient compared to beta-cyclodextrin as an internal reference with known physical diameter of 1.4 nm (see the Supporting Information, Figure S6). Note that the actual size of the CdTeSe alloys might be smaller than 2.3 nm, as hydrodynamic diameters are consistently larger than the actual sizes of nanocrystals because of the contribution from capping ligands, suggested by a systematic study of the comparison of sizes calculated from DOSY and those measured from TEM directly for regular nanocrystals.[40]

4. Conclusion

In summary, novel homogeneously alloyed CdTeSe MSQDs were synthesized via a noninjection one-pot approach. They exhibit bandgap emission at 524 nm with fwhm of ca. 20 nm only and bandgap absorption at 520 nm with the energy difference of its absorption doublet of ca. 288 meV. After their formation during the synthesis, they do not grow any more with longer growth periods and higher reaction temperature. The present discovery opens up a window for the application of facile noninjection methods to produce both alloyed regular and larger MSQD ternary CdTeSe nanocrystals. XRD and ^{113}Cd solid-state NMR demonstrated that they are ternary-alloyed nanocrystals; also, ^{113}Cd solid-state NMR showed that they are homogeneously alloyed rather than gradiently alloyed, with a stoichiometric ratio close to 1Se:1Te, as supported by EDX and XPS. ^{113}Cd solid-state NMR also suggested that each surface Cd atom is attached into the body of the nanocrystal by bonds to two chalcogenides and probably attached to one surface ligand by bonds to the two oxygen atoms of the carboxylate anion. These CdTeSe magic-sized nanocrystals should have practical value in technological applications such as a standard for fluorescence measurements and in fundamental physics to study single-dot optical properties.[4]

Acknowledgment. Ruibing Wang thanks the NRC-Nano Initiative at the National Research Council of Canada for the financial support. The authors thank Dr. Jianying Ouyang for useful discussion on XPS.

Supporting Information Available: The growth kinetics of CdTeSe ternary alloyed MSQDs monitored by the temporal evolution of the absorption and emission of the growing nanocrystals, ^{13}C CP/MAS NMR spectra, EDX elemental analysis table, high-resolution TEM images, and diffusion-ordered NMR spectroscopy (DOSY) for nanocrystal size calculation are included. This material is available free of charge via the Internet at http://pubs.acs.org.

References and Notes

(1) Bruchez, M., Jr.; Moronne, M.; Gin, P.; Weiss, S.; Alivisatos, A. P. *Science* **1998**, *281*, 2013–2016.
(2) Chan, W. C. W.; Nie, S. *Science* **1998**, *281*, 2016–2018.
(3) Han, M.; Gao, X.; Su, J. Z.; Nie, S. *Nat. Biotechnol.* **2001**, *19*, 631–635.
(4) Empedocles, S. A.; Neuhauser, R.; Shimizu, K.; Bawendi, M. G. *Adv. Mater.* **1999**, *11*, 1243–1256.
(5) Schlegel, G.; Bohnenberger, J.; Potapova, I.; Mews, A. *Phys. Rev. Lett.* **2002**, *88*, 137401.
(6) Achermann, M.; Achermann, M.; Petruska, M. A.; Kos, S.; Smith, D. L.; Koleske, D. D.; Klimov, V. I. *Nature* **2004**, *429*, 642–646.
(7) Klimov, V. I.; Mikhailovsky, A. A.; Xu, S.; Malko, A.; Hollingsworth, J. A.; Leatherdale, C. A.; Eisler, H.-J.; Bawendi, M. G. *Science* **2000**, *290*, 315–317.
(8) Eisler, H.-J.; Sundar, V. C.; Bawendi, M. G.; Walsh, M.; Smith, H. I.; Klimov, V. *Appl. Phys. Lett.* **2002**, *80*, 4614.
(9) Murray, C. B.; Norris, D. J.; Bawendi, M. G. *J. Am. Chem. Soc.* **1993**, *115*, 8706–8715.
(10) Peng, Z. A.; Peng, X. *J. Am. Chem. Soc.* **2001**, *123*, 183–184.
(11) Yu, K.; Zaman, B.; Singh, S.; Wang, D.; Ripmeester, J. A. *J. Nanosci. Nanotechnol.* **2005**, *5*, 659–668.
(12) Yang, Y. A.; Wu, H.; Williams, K. R.; Cao, Y. C. *Angew. Chem., Int. Ed.* **2005**, *44*, 6712–6715.
(13) Platschek, V.; Schmidt, T.; Lerch, M.; Muller, G.; Spanhel, L.; Emmerling, A.; Fricke, J.; Foitzik, A. H.; Langer, E. *Ber. Bunsen-Ges. Phys. Chem.* **1998**, *102*, 85.
(14) Peng, Z. A.; Peng, X. *J. Am. Chem. Soc.* **2002**, *124*, 3343–3353.
(15) Cumberland, S. L.; Hanif, K. M.; Javier, A.; Khitrov, G. A.; Strouse, G. F.; Woessner, S. M.; Yun, C. S. *Chem. Mater.* **2002**, *14*, 1576–1584.
(16) Pradhan, N.; Xu, H.; Peng, X. *Nano Lett.* **2006**, *6*, 720–724.
(17) Vossmeyer, T.; Katsikas, L.; Giersig, M.; Popovic, I. G.; Diesner, K.; Chemseddine, A.; Eychmueller, A.; Weller, H. *J. Phys. Chem.* **1994**, *98*, 7665–7673.
(18) Kasuya, A.; Sivamohan, R.; Barnakov, Y. A.; Dmitruk, I. M.; Nirasawa, T.; Romanyuk, V. R.; Kumar, V.; Mamykin, S. V.; Tohji, K.; Jeyadevan, B.; Shinoda, K.; Kudo, T.; Terasaki, O.; Liu, Z.; Belosludov, R. V.; Sundararajan, V.; Kawazoe, Y. *Nat. Mater.* **2004**, *3*, 99–102.
(19) Kudera, S.; Zanella, M.; Giannini, C.; Rizzo, A.; Li, Y.; Gigli, G.; Cingolani, R.; Ciccarella, G.; Spahl, W.; Parak, W. J.; Manna, L. *Adv. Mater.* **2007**, *19*, 548–552.
(20) Dagtepe, P.; Chikan, V.; Jasinski, J.; Leppert, V. J. *J. Phys. Chem. C* **2007**, *111*, 14977–14983.
(21) Soloviev, V. N.; Eichhofer, A.; Fenske, D.; Banin, U. *J. Am. Chem. Soc.* **2001**, *123*, 2354–2364.
(22) Bowers, M. J.; McBride, J. R.; Rosenthal, S. J. *J. Am. Chem. Soc.* **2005**, *127*, 15378–15379.
(23) Evans, C. M.; Guo, L.; Peterson, J. J.; Maccagnano-Zacher, S.; Krauss, T. D. *Nano Lett.* **2008**, *8*, 2896–2899.
(24) Peterson, J. J.; Krauss, T. D. *Nano Lett.* **2006**, *6*, 510–514.
(25) (a) Ouyang, J.; Zaman, Md., B.; Yan, F. J.; Johnston, D.; Li, G.; Wu, X.; Leek, D.; Ratcliffe, C. I.; Ripmeester, J. A.; Yu, K. *J. Phys. Chem. C* **2008**, *112*, 13805–13811. (b) Yu, K.; Ouyang, J.; Badruz, Z.; Johnston, D.; Fu, J. Y.; Li, G.; Ratcliffe, C. I.; Leek, D. M.; Wu, X.; Stupak, J.; Jakubek, Z.; Whitfield, D. *J. Phys. Chem. C* **2009**, DOI: 10.1021/jp809990a.
(26) Wang, R.; Ouyang, J.; Nikolaus, S.; Brestaz, L.; Zaman, M. B.; Wu, X.; Leek, D.; Ratcliffe, C. I.; Yu, K. *Chem. Commun.* **2009**, DOI: 10.1039/b818967f.
(27) Bailey, R. E.; Nie, S. *J. Am. Chem. Soc.* **2003**, *125*, 7100–7106.
(28) Ratcliffe, C. I.; Yu, K.; Ripmeester, J. A.; Zaman, M. B.; Badarau, C.; Singh, S. *Phys. Chem. Chem. Phys.* **2006**, *8*, 3510–3519.
(29) Sachleben, J. R.; Colvin, V.; Emsley, L.; Wooten, E. W.; Alivisatos, A. P. *J. Phys. Chem. B* **1998**, *102*, 10117–10128.
(30) Berrettini, M. G.; Braun, G.; Hu, J. G.; Strouse, G. F. *J. Am. Chem. Soc.* **2004**, *126*, 7063–7070.
(31) Ladizhansky, V; Hodes, G; Vega, S. J. *Phys. Chem. B* **1998**, *102*, 8505–8509.
(32) Elbaum, R.; Vega, S.; Hodes, G. *Chem. Mater.* **2001**, *13*, 2272–2280.
(33) Lo, A. Y. H.; Sudarsan, V.; Sivakumar, S.; van Veggel, F.; Schurko, R. W. *J. Am. Chem. Soc.* **2007**, *129*, 4687–4700.

(34) Holland, G. P.; Sharma, R.; Agola, J. O.; Amin, S.; Solomon, V. C.; Singh, P.; Buttry, D. A.; Yarger, J. L. *Chem. Mater.* **2007**, *19*, 2519–2526.

(35) Ouyang, J.; Ratcliffe, C. I.; Kingston, D.; Wilkinson, B.; Kuijper, J.; Wu, X.; Ripmeester, J. A.; Yu, K. *J. Phys. Chem. C* **2008**, *112*, 4908–4919.

(36) Harrison, W.; Trotter, J. *J. Chem. Soc. Dalton Trans.* **1972**, 956–960.

(37) Stamatatos, T. C.; Katsoulakou, E.; Nastopoulos, V.; Raptopoulou, C. P.; Manessi-Zoupa, E.; Perlepes, S. P. *Z. Naturforsch.* **2003**, *58b*, 1045–1054.

(38) Choi, K.-Y.; Jeon, Y.-M.; Lee, K.-C.; Ryu, H.; Suh, M.; Park, H.-S.; Kim, M.-J.; Song, Y.-H. *J. Chem. Crystallog.* **2004**, *34*, 591–595.

(39) Poul, L.; Fakhfakh, M.; Taibi, M.; Jouini, N.; Herson, P.; Fievet, F. *J. Chem. Crystallog.* **2005**, *35*, 285–291.

(40) Hens, Z.; Moreel, I.; Martins, J. C. *ChemPhysChem* **2005**, *6*, 2578–2584.

(41) Shen, L.; Soong, R.; Wang, M.; Lee, A.; Wu, C.; Scholes, G. D.; Macdonald, P. M.; Winnik, M. A. *J. Phys. Chem. B* **2008**, *112*, 1626–1633.

JP810325Z